Electromagnetic transition probabilities in the natural-parity rotational band of ^{173}Yb

M. Oshima, M. Matsuzaki,* S. Ichikawa, and H. Iimura
Japan Atomic Energy Research Institute, Tokai-mura, Naka-gun, Ibaraki 319-11, Japan

H. Kusakari
Chiba University, Yayoi-cho, Chiba 260, Japan

T. Inamura and A. Hashizume
The Institute of Physical and Chemical Research (RIKEN), Wako-shi, Saitama 351-01, Japan

M. Sugawara
Chiba Institute of Technology, Shibazono, Narashino-shi, Chiba 275, Japan
(Received 14 June 1989)

The ground-state rotational band of ^{173}Yb has been investigated through multiple Coulomb excitation with a beam of 250-MeV ^{58}Ni. γ-ray branchings and $E2/M1$ mixing ratios were determined up to the $\frac{23}{2}^-$ state by measurements of γ-ray angular distributions and γ-γ angular correlations. Nuclear lifetimes of levels up to $I=\frac{25}{2}$ have been measured using the Doppler-shift recoil-distance method. No significant signature dependence was observed for $\Delta I=1$ $M1$ and $E2$ transition probabilities. The data are analyzed in terms of the rotating shell model and the differences between spin-up and spin-down orbitals are discussed.

I. INTRODUCTION

Electromagnetic transition probabilities have been studied especially for the rotational bands based on high-j orbitals such as $h_{11/2}$ or $i_{13/2}$.[1-7] These high-j orbitals have a unique-parity character, and there is less ambiguity about the wave function than in the case of natural-parity orbitals. Rotational perturbations are strong for the unique-parity bands, and considerable signature dependence (zigzag pattern) has been observed for the quasiparticle energy and the $B(M1)$ values. The phase rule[8] for the zigzag patterns is well established for the unique-parity bands.

In the natural-parity rotational band of ^{163}Dy we have found that the phase of the zigzag in the $B(M1)$ values is opposite to the one which is expected for the dominant $j=\frac{9}{2}$ configuration,[9,10] while the quasiparticle energy splitting and the absolute value of the $B(M1)$ are in agreement with the dominant $j=\frac{9}{2}$ character for this band. The "inverted" signature dependence was shown in terms of the rotating shell model to originate from the characteristic coherence between the orbital and spin contributions in the spin-down ($\Omega=\Lambda-\frac{1}{2}$) dominant one-quasiparticle states.[10,11] In order to confirm such a mechanism, the counterpart, i.e., the spin-up ($\Omega=\Lambda+\frac{1}{2}$) dominant configurations should be studied.

Because of this we undertook a Coulomb-excitation experiment on ^{173} Yb whose ground-state rotational band is based on the natural-parity Nilsson state $\nu\frac{5}{2}$ [512]. We have assigned levels up to $J^\pi=(\frac{27}{2}^-)$ and measured γ-ray branchings, $E2/M1$ mixing ratios, and nuclear lifetimes, and determined the absolute intraband transition probabilities up to the $\frac{25}{2}^-$ state. The levels of ^{173}Yb have been investigated so far through (n,γ) (Ref. 12), (d,t) (Ref. 13), (d,p) (Refs. 13 and 14), and Coulomb excitation by light ions (Refs. 15–17). From these works the ground band has been known up to $I=\frac{13}{2}$, and lifetimes of the ground-band members were known up to the second excited state $\frac{9}{2}^-$ (Ref. 18).

II. EXPERIMENTAL PROCEDURE AND RESULTS

A self-supporting metallic target of ^{173}Yb (92.1% enriched and about 30 mg/cm^2 thick) was bombarded with a beam of 250-MeV ^{58}Ni from the tandem accelerator at Japan Atomic Energy Research Institute. The target nucleus ^{173}Yb was multiply Coulomb excited by the beam, which was stopped in the target.

In γ-γ coincidence measurements, three Compton-suppression γ-ray spectrometers[19] were placed at 0°, 90°, and −90° to the beam. The distance between the target and the detectors was 7 cm. The data acquisition was controlled by a VAX-780 computer, and all events were recorded on magnetic tapes for later analysis. A sum of the coincidence spectra gated for ground-band members is shown in Fig. 1. Levels up to the one at 2018 keV were established in the coincidence spectra as presented in Fig. 2.

Angular distributions of γ rays were measured with a Compton-suppression spectrometer at seven angles between 0° and 90° to the beam direction. The distance between the target and the spectrometer was 10 cm.

The angular distributions were fitted with Legendre polynomials

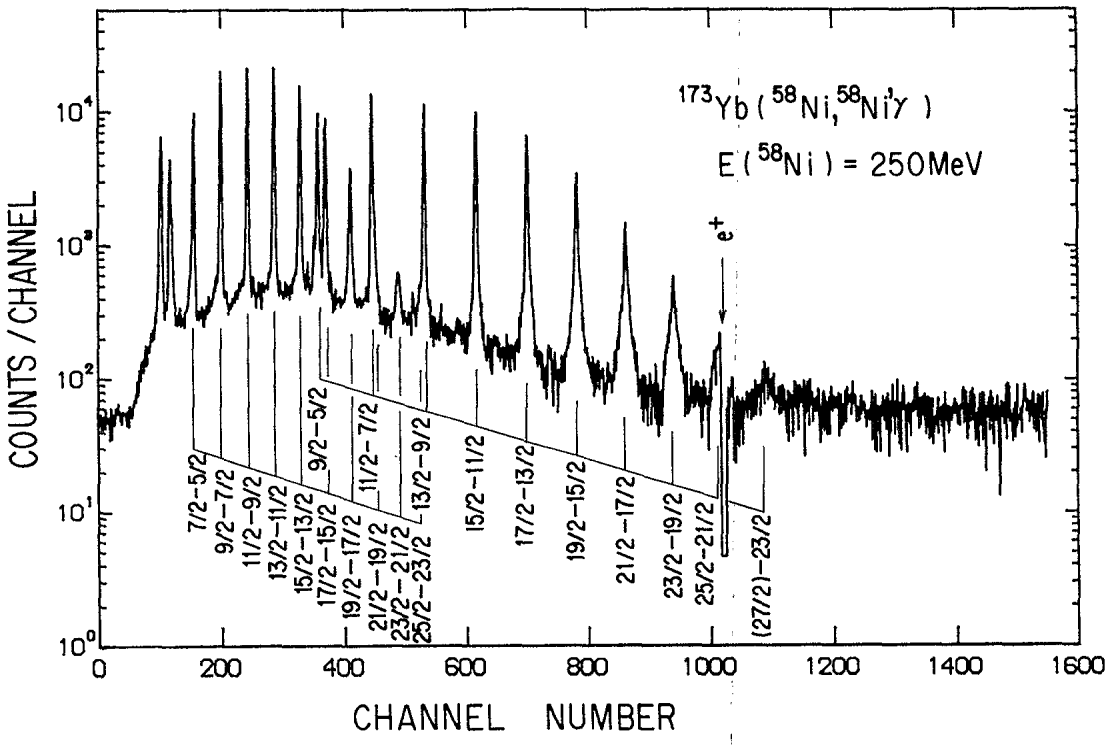

FIG. 1. A sum of coincidence spectra gated by ground-band members of ^{173}Yb.

$$W(\theta)=A_0(1+A_2Q_2P_2(\cos\theta)+A_4Q_4P_4(\cos\theta)) \ . \quad (1)$$

The Q_2 and Q_4 values are the geometrical attenuation factors. For the detector configuration used, the Q_2 and Q_4 were estimated for each γ ray energy from Ref. 20. The derived coefficients A_2 and A_4 are presented in Table I. We evaluated the degree of alignment for each state, i.e., alignment attenuation factors,[21] α_2 and α_4: The experimental A_2 values of the $\Delta I=2$ transitions give the alignment attenuation factor, α_2, for the decaying states because these transitions are of pure $E2$; α_4 was estimated from α_2 by assuming a Gaussian distribution of magnetic-substate population. An $E2/M1$ mixing ratio for a $\Delta I=1$ transition is derived from the attenuation factors for the state of interest and the angular-distribution coefficients. The γ-ray intensities derived from the γ-ray angular-distribution analyses are presented in Table I.

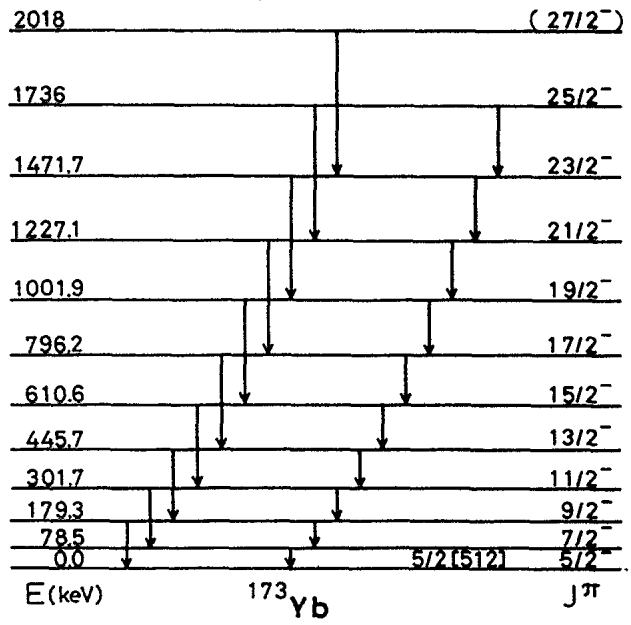

FIG. 2. A level scheme of the ground-state rotational band of ^{173}Yb.

Lifetime measurements were made by the Doppler-shift recoil-distance method. In this case, the target thickness was 2.1 mg/cm^2. Back-scattered projectiles were measured with a plastic annular scintillator which subtended an angle range of $\theta_{lab}=150°-175°$ to the beam direction. γ-ray spectra in coincidence with the back-scattered projectiles were measured with a Compton-suppression γ-ray spectrometer placed at 0° to the beam. The distance between the target and the spectrometer was 13 cm. The average value of the recoil velocity that was determined from the positions of shifted and unshifted γ-ray peaks was 10.5 ± 0.8 μm/ps, which corresponds to $(0.0350\pm0.0027)c$, c being the velocity of light. The coincidence spectra were measured for 14 recoil distances ranging from 15 μm to 8.28 mm. The electric pulse height, which reflects capacitance between the target and stopper, was monitored during the measurements.

Figure 3 shows particle-gated γ-ray spectra taken at four recoil distances. Shifted and unshifted intensities were derived from the spectra. Figure 4 shows plots of the unshifted intensity versus the recoil distance, i.e., decay curves for excited states. Data on the shifted and un-

TABLE I. Summary of γ transitions in the ground-state rotational band of ^{173}Yb. E_γ is γ-ray energy. I_γ denotes the relative γ-ray intensity which was corrected for angular distributions. I_{total} indicates the total intensity corrected for internal conversions. A_2 and A_4 are γ-ray angular-distribution coefficients. δ is the $E2/M1$ mixing ratio. Figures in parentheses denote uncertainties.

J_i	J_f	E_γ (keV)	I_γ	I_{total}	A_2	A_4	δ
$\frac{7}{2}$	$\frac{5}{2}$	78.5(1)	100(2)	805(16)	−0.002(8)	0.05(4)	−0.237(7)[a]
$\frac{9}{2}$	$\frac{7}{2}$	100.8(1)	58.4(11)	264(5)	−0.061(8)	0.012(11)	−0.205(20)[a]
$\frac{9}{2}$	$\frac{5}{2}$	179.3(1)	16.1(3)	22.4(4)	0.010(8)	0.011(10)	
$\frac{11}{2}$	$\frac{9}{2}$	122.4(1)	22.7(4)	66.5(13)	−0.181(8)	0.020(10)	−0.22(6)
$\frac{11}{2}$	$\frac{7}{2}$	223.2(1)	14.6(3)	17.4(3)	0.115(8)	−0.035(10)	
$\frac{13}{2}$	$\frac{11}{2}$	144.0(1)	11.3(2)	25.1(5)	−0.242(8)	0.013(10)	−0.15(4)
$\frac{13}{2}$	$\frac{9}{2}$	266.4(1)	12.1(2)	13.4(3)	0.176(8)	−0.001(10)	
$\frac{15}{2}$	$\frac{13}{2}$	164.9(1)	5.30(11)	9.7(2)	−0.243(8)	−0.009(10)	−0.12(4)
$\frac{15}{2}$	$\frac{11}{2}$	308.9(1)	8.11(16)	8.65(17)	0.199(8)	0.005(11)	
$\frac{17}{2}$	$\frac{15}{2}$	185.6(1)	1.78(3)	2.83(6)	−0.294(8)	0.008(10)	−0.15(4)
$\frac{17}{2}$	$\frac{13}{2}$	350.5(1)	4.96(15)	5.20(15)	0.208(8)	−0.002(11)	
$\frac{19}{2}$	$\frac{17}{2}$	205.7(1)	0.77(3)	1.14(4)	−0.402(12)	0.031(16)	−0.20(4)
$\frac{19}{2}$	$\frac{15}{2}$	391.3(1)	2.99(6)	3.08(6)	0.249(8)	−0.084(11)	
$\frac{21}{2}$	$\frac{19}{2}$	225.2(1)	0.238(11)	0.32(2)	−0.499(26)	0.05(3)	−0.18(7)
$\frac{21}{2}$	$\frac{17}{2}$	430.9(1)	1.47(3)	1.51(3)	0.329(9)	−0.095(11)	
$\frac{23}{2}$	$\frac{21}{2}$	244.6(1)	0.108(16)	0.14(2)	−0.51(7)	0.08(9)	−0.18(18)
$\frac{23}{2}$	$\frac{19}{2}$	469.8(1)	0.70(3)	0.71(3)	0.353(15)	−0.130(20)	
$\frac{25}{2}$	$\frac{21}{2}$	508.9(3)	0.4(2)	0.4(2)	0.30(21)	0.0(3)	
$\frac{27}{2}$	$\frac{23}{2}$	546.3(3)					

[a]From Ref. 18.

shifted intensities were analyzed by a computer program "LIFETIME."[22] The fitted results are shown in Fig. 4. The Coulomb-excitation process does not cause any serious side-feeding contribution to the decay curves, which often brings considerable uncertainty of the final result in compound nuclear residues. This feature enables the lifetimes of excited states to be determined accurately.

The lifetimes obtained for the states from $\frac{9}{2}$ to $\frac{25}{2}$ are summarized in Table II. The reduced transition probabilities are plotted in Figs. 5–7.

TABLE II. Summary of lifetimes and reduced transition probabilities.

I	τ (ps)	$B(E2;I\rightarrow I-2)$ (e^2b^2)	$B(M1;I\rightarrow I-1)$ (μ_N^2)	$B(E2;I\rightarrow I-1)$ (e^2b^2)
$\frac{7}{2}$	75(9)[a]		0.184(23)[b]	2.42(33)[c]
$\frac{9}{2}$	41(4)[c]	0.61(6)[c]	0.264(27)[d]	1.58(34)[d]
$\frac{11}{2}$	24.1(21)	1.07(10)	0.332(31)	1.6(8)
$\frac{13}{2}$	17.6(15)	1.09(10)	0.310(28)	0.49(26)
$\frac{15}{2}$	10.6(9)	1.22(11)	0.341(30)	0.26(17)
$\frac{17}{2}$	6.2(5)	1.54(14)	0.31(6)	0.29(16)
$\frac{19}{2}$	3.7(3)	1.72(18)	0.31(3)	0.43(17)
$\frac{21}{2}$	2.61(23)	1.69(15)	0.239(25)	0.22(17)
$\frac{23}{2}$	1.66(24)	1.76(27)	0.29(6)	0.22(44)
$\frac{25}{2}$	0.86(7)	1.6(7)		

[a]From Ref. 15.
[b]Deduced from $B(E2;\frac{7}{2}\rightarrow\frac{5}{2})$ and $\delta=-0.237(7)$ (Ref. 18).
[c]From Ref. 16.
[d]Deduced from $B(E2;\frac{9}{2}\rightarrow\frac{5}{2})$, branching and mixing ratios (Ref. 18).

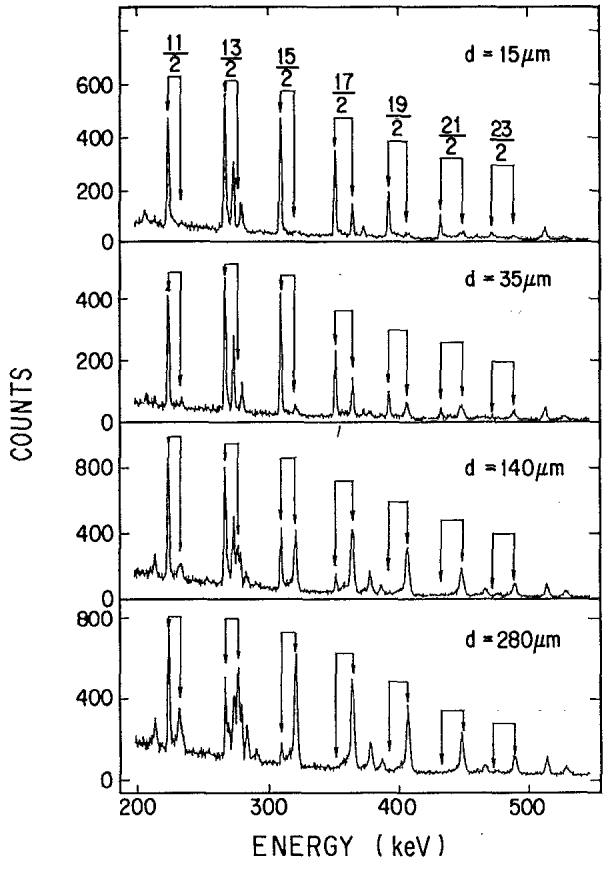

FIG. 3. Illustrative particle-gated γ-ray spectra of ^{173}Yb covering the 190–560 keV region for four of the 14 recoil distances measured.

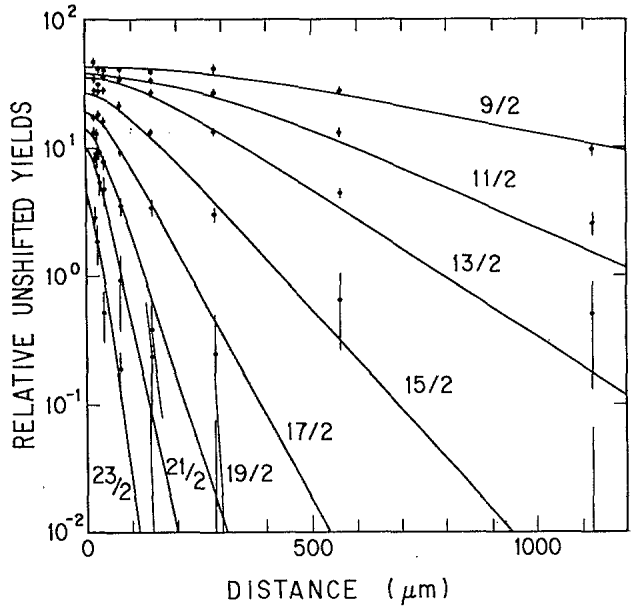

FIG. 4. Decay curves for the ground-band members of ^{173}Yb. The intensities were summed for $\Delta I=1$ and $\Delta I=2$ transitions depopulating each state.

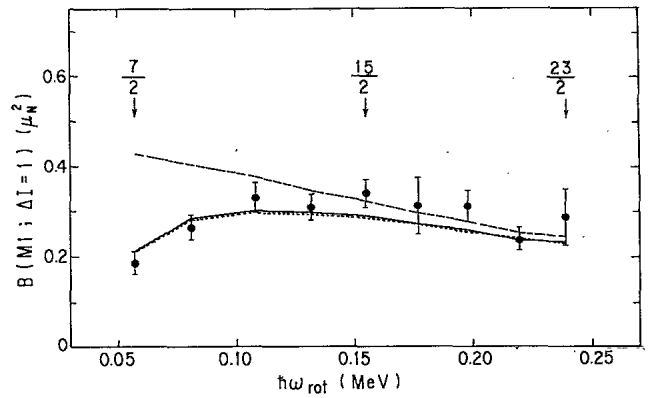

FIG. 5. $B(M1;I\rightarrow I-1)$ values for the ground-state rotational band of ^{173}Yb. The experimental values for $I=\frac{7}{2}$ and $\frac{9}{2}$ are from Ref. 18, and others are the present data. The solid (dashed) line shows the calculation with (without) the geometrical factor. The dotted line includes the γ vibration besides the geometrical factor.

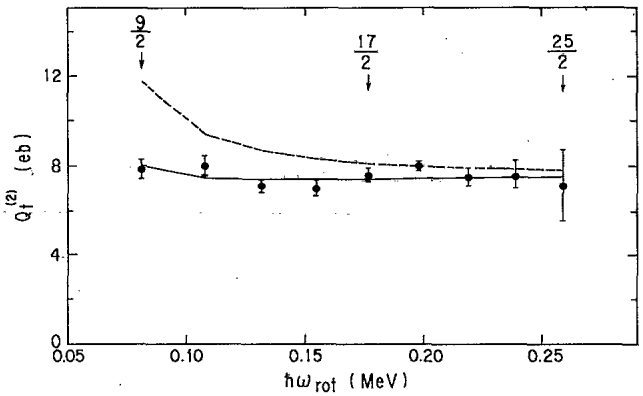

FIG. 6. $\Delta I=1$ transition quadrupole moments for the ground-state rotational band of ^{173}Yb. They are defined as follows (Ref. 23):

$$Q_t^{(\Delta I)}=\{B(E2;I\rightarrow I-\Delta I)/[(5/16\pi)\langle I2K0|I-\Delta IK\rangle^2]\}^{1/2},$$

where $K=\frac{5}{2}$ was assumed. The experimental values for $I=\frac{7}{2}$ and $\frac{9}{2}$ are from Refs. 16 and 18, respectively, and others are the present data. The solid and dashed lines denote the present rotating-shell-model calculation, which were obtained using an aligned angular momentum $i_x=0.8$; the notations for the solid and dashed lines are the same as in Fig. 5.

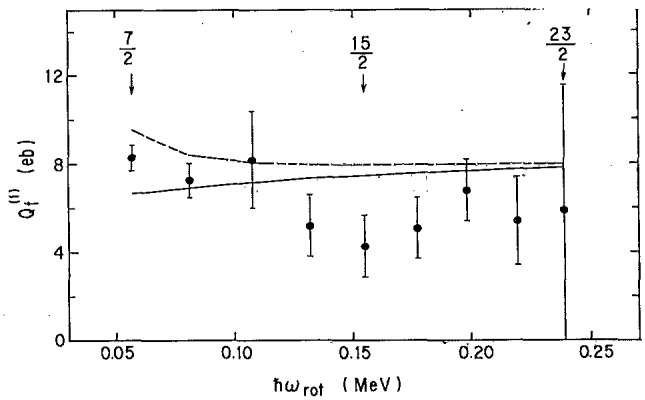

FIG. 7. $\Delta I=2$ transition quadrupole moments for the ground-state rotational band of ^{173}Yb. The experimental value for $I=\frac{9}{2}$ is from Ref. 16, and others are the present data. The notations for the solid and dashed lines are the same as in Fig. 5.

III. THEORETICAL CALCULATION

We performed microscopic theoretical calculation based on the rotating shell model.[24] In this framework, account is taken of many important physical mechanisms: static and dynamic triaxial deformations which are appreciated to be important in the case of unique-parity orbitals,[25] the many-j mixing effect which is crucial in treating natural-parity orbitals,[10,11] and many-quasiparticle configurations[26] which may become yrast at very high spins. On the other hand, this framework becomes worse at low-spin states because of its semiclassical nature. In order to overcome this defect in a simple manner, we adopted the "geometrical factors" proposed by Dönau.[27] The details are given in the Appendix.

The parameters used in the numerical calculation were determined as follows. We used the single-particle space consisting of the $N_{\rm osc}=4-6$ major shells for neutrons and the $N_{\rm osc}=3-5$ shells for protons. Here we note that our model space includes all the j components which can be contained in the odd-quasineutron orbital under consideration. Quadrupole deformation parameter $\delta=0.28$ was chosen so as to approximately reproduce the observed quadrupole moments of neighboring even-even nuclei[28] using the experimental pairing gaps $\Delta_n=0.703$ MeV and $\Delta_p=0.894$ MeV, and the chemical potentials which gave the correct particle numbers at zero rotational frequency, i.e., $\hbar\omega_{\rm rot}=0$. The static triaxial parameter was set to zero because we confirmed, by using the isotropic-velocity-distribution condition,[29] that the equilibrium triaxial deformation was smaller than 3°. We used the average aligned angular momentum $i_x=0.8$, extracted from the experimental data, when we evaluated $B(E2;\Delta I=1)$ values.[10] Effective spin g factor $g_s^{(\rm eff)}=0.87\ g_s^{(\rm free)}$ [Ref. 23] was used.

For the random-phase approximation (RPA) and quasiparticle-vibration-coupling calculations, the strengths of the doubly-stretched quadrupole interaction were fixed at $\hbar\omega_{\rm rot}=0$ to reproduce the excitation energies of the lowest $K=0$ and 2 vibrational states in the adjacent even-even nuclei,[30] and to restore the broken rotational invariance. The pairing force strengths were determined at the same time with the chemical potentials by utilizing the BCS equations at each rotational frequency. Gamma-vibrational phonons ($r=\pm1$) were taken into account up to double excitations. The calculated results with and without the geometrical factors are presented in Figs. 5–7.

IV. DISCUSSION

All of the observed quantities, level energies, $B(M1)$, $B(E2;\Delta I=1)$, and $B(E2;\Delta I=2)$, show almost no signature dependence. This appears natural for spin-up ($\Omega=\Lambda+\frac{1}{2}$) dominant one-quasiparticle bands with natural parity,[11] and our calculation reproduces them very well. The spin-up character in the present case is mainly due to the $f_{7/2}$ spherical-shell-model state. Namely, the orbital under consideration $\nu\frac{5}{2}$ [512] is the counterpart to the $\nu\frac{5}{2}$ [523], whose dominant component is $h_{9/2}$ after an avoided crossing, occupied by the last odd particle of ^{163}Dy.[10]

Since the signature dependence is negligibly weak and the absolute values of $B(E2)$ are determined by the Clebsh-Gordan coefficients after a deformation parameter is fixed, the most important physical quantity is the absolute value of $B(M1)$. It is determined by $|g_j-g_{\rm RPA}|$ in the rotating shell model when one of the spherical-shell-model states j is dominant in the deformed wave function. Here g_j is the Schmidt value with $g_s^{(\rm eff)}$ and $g_{\rm RPA}$ is calculated as[11]

$$g_{\rm RPA}=\frac{\langle\mu_x\rangle}{\langle J_x\rangle}\ . \tag{2}$$

Consequently the absolute values of $B(M1)$ are large (small) when g_j is negative (positive) in one-quasiparticle bands where $g_{\rm RPA}$ is positive. Besides the calculation within the rotating shell model, the vibrational contributions are expected to affect the $B(M1)$ value depending on the shell structure.[10] Here we discuss the role of γ vibration in the present case.

The phenomenological g_R is extracted from experimental data using a model without the vibrational contributions.[23] When the contributions are negligible, the calculated $g_{\rm RPA}$ and the phenomenological g_R should coincide with each other and the $B(M1)$ value should be reproduced within the rotating shell model. This holds well in the present case of ^{173}Yb (Fig. 5), where the calculated $g_{\rm RPA}$ varies from 0.292 to 0.283 as the rotational frequency increases, whereas the phenomenological g_R is 0.277 ± 0.017.[31] This result is consistent with the fact that the collectivity of γ vibration is very weak around the nucleus ^{173}Yb due to the subshell structure in the Nilsson orbitals.[23] In contrast, the calculated values of $g_{\rm RPA}$ were considerably larger than the phenomenological g_R and consequently the calculated $B(M1)$ values were larger than the experimental ones in the case of ^{163}Dy.[10] But this discrepancy has been solved by taking the γ-vibrational effects into account.[10]

Although the relation between magnetic properties and triaxiality is not straightforward, a possible interpretation is as follows: The coupling between the odd-quasineutron and the γ-vibrational excitation reduces the degree of time-reversal symmetry between the signature-partner states, i.e., the neutron pairing correlation is reduced effectively; and consequently the moment of inertia of neutron parts increases and the g factor of the core rotor decreases so as to reduce the $B(M1)$ values.

Transition quadrupole moments deduced from $B(E2)$ values are shown in Figs. 6 and 7. Our rotating-shell-model calculation reproduces them well. This means that the adopted deformation parameter is adequate. The effects of the γ vibration on them have been found to be negligible.

V. SUMMARY

The electromagnetic transition properties in the natural-parity ground-state rotational band of ^{173}Yb have been studied experimentally and theoretically. All of the observed quantities show almost no signature dependence

as generally expected for the spin-up one-quasiparticle bands with natural parity. Our rotating-shell-model calculations reproduce both the absolute values and the signature dependence of these quantities well. The effects of γ vibration on them are shown to be negligibly small as expected from the subshell structure in the Nilsson orbitals. It is also pointed out that the effects of residual interactions between quasiparticles are important in order to describe the electromagnetic properties irrespective of the collectivity of γ vibration by referring to our previous result for ^{163}Dy.

ACKNOWLEDGMENTS

We are indebted to Dr. Y. R. Shimizu for providing the rotating-shell-model wave function. We would also like to thank Dr. N. Shikazono and Dr. H. Kamitsubo for their support of this study. This study has been carried out as a joint research program between Japan Atomic Energy Research Institute (JAERI) and RIKEN.

APPENDIX

The rotating-shell-model approach to odd-A nuclei becomes worse at low-spin states because of the deviation between the direction of the total angular momentum and the cranking axis. The model of Matsuzaki, Shimizu, and Matsuyanagi gives a method to construct the principal-axis (PA) frame operators which act on the rotating-shell-model wave functions, and describes *the signature dependence* of transition rates well.[24] But it overestimates *the absolute magnitudes* of them at low-spin states since the geometrical effect mentioned above is not incorporated in it. Dönau proposed a simple method to take such an effect into account assuming that the PA-frame operators were known.[27] The essential virtue of his method is to improve the absolute magnitudes of transition rates although it may alter the signature dependence slightly. To inherit this virtue in the model of Matsuzaki *et al.* phenomenologically, we simply multiply each PA-frame operator given in Refs. 24 and 10 by a geometrical factor as follows:

$$\hat{\mu}_{-1}^{(\mathrm{geom})} = \left[1-\left[\frac{K}{I}\right]^2\right]^{1/2} \hat{\mu}_{-1}^{(\mathrm{PA})} ,$$
$$\hat{Q}_{2-1}^{(\mathrm{geom})} = \left[1-\left[\frac{K}{I}\right]^2\right]^{1/2} \hat{Q}_{2-1}^{(\mathrm{PA})} \qquad \text{(A1)}$$
$$\hat{Q}_{2-2}^{(\mathrm{geom})} = \left[1-\left[\frac{K}{I}\right]^2\right] \hat{Q}_{2-2}^{(\mathrm{PA})} ,$$

where K is the angular momentum projection onto the symmetry axis and assumed to be $\frac{5}{2}$ in the present case.

*Present address: Institute of Physics, University of Tsukuba, Tsukuba, Ibaraki 305, Japan.

[1]G. B. Hagemann, J. D. Garrett, B. Herskind, J. Kownacki, B. M. Nyakó, P. L. Nolan, J. F. Sharpey-Schafer, and P. O. Tjøm, Nucl. Phys. **A424**, 365 (1984); D. C. Radford, H. R. Andrews, G. C. Ball, D. Horn, D. Ward, F. Banville, S. Flibotte, P. Taras, J. Johansson, D. Tucker, and J. C. Waddington, Proceedings of the Workshop on Nuclear Structure, Copenhagen, 1988 (unpublished).

[2]M. Ohshima, E. Minehara, M. Ishii, T. Inamura, and A. Hashizume, Nucl. Phys. **A436**, 518 (1985).

[3]K. Honkanen, H. C. Griffin, D. G. Sarantites, V. Abenante, L. A. Adler, C. Baktash, Y. S. Chen, O. Dietzsch, M. L. Halbert, D. C. Hensley, N. R. Johnson, A. J. Larabee, I. Y. Lee, L. L. Riedinger, J. X. Saladin, T. M. Semkow, and Y. Schutz, in *Nuclei off the Line of Stability,* ACS Symposium Series No. 324, edited by R. A. Meyer and D. S. Brenner (American Chemical Society, Washington, D.C., 1986), p. 317.

[4]J. Gascon, P. Taras, D. C. Radford, D. Ward, H. R. Andrews, and F. Banville, Nucl. Phys. **A467**, 539 (1987).

[5]C.-H. Yu, M. A. Riley, J. D. Garrett, G. B. Hagemann, J. Simpson, P. D. Forsyth, A. R. Mokhtar, J. D. Morrison, B. M. Nyakó, J. F. Sharpey-Schafer, and R. Wyss, Nucl. Phys. **A489**, 477 (1988).

[6]P. Frandsen, R. Chapman, J. D. Garrett, G. B. Hagemann, B. Herskind, C.-H.Yu, K. Schiffer, D. Klarke, F. Khazaie, J. C. Lisle, J. N. Mo, L. Carlén, P. Ekström, and H. Ryde, Nucl. Phys. **A489**, 508 (1988).

[7]M. Oshima, E. Minehara, S. Ichikawa, H. Iimura, T. Inamura, A. Hashizume, H. Kusakari, and S. Iwasaki, Phys. Rev. C **37**, 2578 (1988).

[8]I. Hamamoto, Phys. Lett. **106B**, 281 (1981); in *Proceedings of the Niels Bohr Centennial Conference on Nuclear Structure, Copenhagen 1985,* edited by R. Broglia, G. B. Hagemann, and B. Herskind (North-Holland, Amsterdam, 1985) p. 129.

[9]E. Minehara, M. Oshima, S. Kikuchi, T. Inamura, A. Hashizume, and H. Kumahora, Phys. Rev. C **35**, 858 (1987).

[10]M. Oshima, E. Minehara, S. Kikuchi, T. Inamura, A. Hashizume, H. Kusakari, and M. Matsuzaki, Phys. Rev. C **39**, 645 (1989).

[11]M. Matsuzaki, Phys. Rev. C **39**, 691 (1989).

[12]G. Alenius, S. E. Arnell, C. Schale, and E. Wallander, Nucl. Phys. **A161**, 209 (1971).

[13]D. G. Burke, B. Zeidman, B. Eldek, B. Herskind, and M. Olesen, K. Dan. Vidensk. Selsk. Mat.-Fys. Medd. **35**, No. 2 (1966).

[14]J. Gastebois, B. Fernandez, and J. M. Laget, Nucl. Phys. **A125**, 531 (1969).

[15]Y. Dar, J. Berger, A. Macher, and J. P. Vivien, Nucl. Phys. **A171**, 575 (1971).

[16]B. Elbek, Ph.D. thesis, University of Copenhagen, 1963.

[17]J. M. Palms, E. M. Bernstein, and G. G. Seaman, Phys. Rev. **151**, 1004 (1966).

[18]B. Harmatz and D. J. Horen, Nucl. Data Sheets **14**, 297 (1975).

[19]E. Minehara, M. Oshima, T. Inamura, A. Hashizume, and H. Kumahora, in Proceedings of the International Symposium on Nuclear Spectroscopy and Nuclear Interactions, Osaka, 1984, edited by H. Ejiri and T. Fukuda (unpublished).

[20]D. C. Camp and A. L. Van Lehn, Nucl. Instrum. Methods **76**, 192 (1969).

[21]H. Morinaga and T. Yamazaki, *In-Beam Gamma-Ray Spectroscopy* (North-Holland, Amsterdam, 1976).

[22]J. C. Wells, M. P. Fewell, and N. R. Johnson, *Oak Ridge Na-*

tional Laboratory Report ORNL/TM-9105, 1985.
[23]A. Bohr and B. R. Mottelson, *Nuclear Structure* (Benjamin, New York, 1975), Vol. 2.
[24]M. Matsuzaki, Y. R. Shimizu, and K. Matsuyanagi, Prog. Theor. Phys. **79**, 836 (1988).
[25]M. Matsuzaki, Nucl. Phys. **A491**, 433 (1989), and references therein.
[26]M. Matsuzaki, Y. R. Shimizu, and K. Matsuyanagi, Prog. Theor. Phys. **77**, 1302 (1987).
[27]F. Dönau, Nucl.Phys. **A471**, 469 (1987).
[28]K. E. G. Löbner, M. Vetter, and V. Hönig, Nucl. Data Tables **A7**, 495 (1970).
[29]Y. R. Shimizu and K. Matsuyanagi, Prog. Theor. Phys. **71**, 960 (1984).
[30]M. Sakai, At. Data Nucl. Data Tables **31**, 399 (1984).
[31]F. Boehm, G. Goldring, G. B. Hagemann, G. D. Symons, and A. Tveter, Phys. Lett. **22**, 627 (1966).